BIOCHEMISTRY
including biophysical chemistry & molecular biology
Article

Biochemistry **2009,** *48,* 9801–9809 9801
DOI: 10.1021/bi901024m

Disruption of the Proton Relay Network in the Class 2 Dihydroorotate Dehydrogenase from *Escherichia coli*†

Rebecca L. Kow,[‡,∥] Jonathan R. Whicher,[§] Claudia A. McDonald,[‡] Bruce A. Palfey,[‡,§] and Rebecca L. Fagan*[,‡,⊥]

[‡]*Department of Biological Chemistry, University of Michigan Medical School, Ann Arbor, Michigan 48109-5606, and* [§]*Doctoral Program in Chemical Biology, University of Michigan, Ann Arbor, Michigan 48109* [∥]*Present address: Department of Pharmacology, University of Washington Medical School, Seattle, WA 98195-7280.* [⊥]*Present address: Department of Biochemistry, University of Iowa, Iowa City, IA 52242-1109.*

Received June 17, 2009; Revised Manuscript Received July 29, 2009

ABSTRACT: Dihydroorotate dehydrogenases (DHODs) are FMN-containing enzymes that catalyze the conversion of dihydroorotate (DHO) to orotate in the de novo synthesis of pyrimidines. During the reaction, a proton is transferred from C5 of DHO to an active site base and the hydrogen at C6 of DHO is transferred to N5 of the isoalloxazine ring of the flavin as a hydride. In class 2 DHODs, a hydrogen bond network observed in crystal structures has been proposed to deprotonate the C5 atom of DHO. The active site base (Ser175 in the *Escherichia coli* enzyme) hydrogen bonds to a crystallographic water molecule that sits on a phenylalanine (Phe115 in the *E. coli* enzyme) and hydrogen bonds to a threonine (Thr178 in the *E. coli* enzyme), residues that are conserved in class 2 enzymes. The importance of these residues in the oxidation of DHO was investigated using site-directed mutagenesis. Mutating Ser175 to alanine had severe effects on the rate of flavin reduction, slowing it by more than 3 orders of magnitude. Changing the size and/or hydrophobicity of the residues of the hydrogen bond network, Thr178 and Phe115, slowed flavin reduction as much as 2 orders of magnitude, indicating that the active site base and the hydrogen bond network work together for efficient deprotonation of DHO.

Dihydroorotate dehydrogenases (DHODs)[1] catalyze the fourth step in the de novo synthesis of pyrimidines. DHODs are flavin-containing enzymes that convert dihydroorotate (DHO) to orotate (OA), the only redox step in pyrimidine synthesis (Scheme 1). DHODs have been categorized into two broad classes based on sequence (*1*). Class 2 DHODs are membrane-bound monomers that are oxidized by ubiquinone (*2*). Class 1 DHODs are cytosolic proteins that have been further divided into two classes. Class 1A DHODs are homodimers that use fumarate as the physiological oxidizing substrate (*3*). Class 1B DHODs are $\alpha_2\beta_2$ heterotetramers. One subunit resembles the class 1A monomer, and a second subunit contains an iron−sulfur cluster and FAD, allowing the class 1B DHODs to be oxidized by NAD (*4*). Class 2 DHODs are found in most eukaryotes and Gram-negative bacteria, while class 1 enzymes are found mostly in Gram-positive bacteria and in a few microbial eukaryotes.

All DHODs catalyze the same reductive half-reaction, the oxidation of DHO with the concomitant reduction of the enzyme-bound flavin, while the oxidative half-reactions for each class are different. Structures of class 2 DHODs have shown that the enzymes contain two separate substrate-binding sites (*5*−*10*). The pyrimidine-binding site is found on the *si* face of the flavin and is very similar in all DHODs. The quinone-binding site is thought to be in a tunnel-like pocket (formed by an N-terminal domain found only in class 2 DHODs) that leads to the 7,8-dimethyl edge of FMN.

Oxidation of DHO breaks two carbon−hydrogen bonds. An active site base (serine in class 2 enzymes or cysteine in class 1 enzymes) deprotonates C5 of DHO, and a hydride is transferred from C6 of DHO to N5 of the isoalloxazine ring of the flavin. The reductive half-reaction of the class 2 DHOD from *Escherichia coli* has been studied in great detail in anaerobic stopped-flow experiments. The rate constant for reduction increased with pH until it plateaued above a pK_a of ∼9.5 (*11*). Structures show that a serine is positioned to deprotonate DHO (*7*−*9*). However, there are no obvious structural features that would lower the pK_a so dramatically (a change of four pH units or more) from that of an unactivated serine. Deuterium isotope effects showed that DHO oxidation occurs in a stepwise fashion in class 2 DHODs (*12*). In addition, using DHO deuterated at the C5 position (the site of deprotonation), the kinetic isotope effect was lost at a pH value above the pK_a (*12*), leading to the proposal that the observed pK_a in class 2 DHODs is actually a kinetic pK_a. Thus, at sufficiently high pH values, the rate constant for DHO deprotonation becomes so much larger than that of hydride transfer that it is not even partially rate-determining in the overall observed rate constant for reduction.

Crystal structures show that the active site base is part of a hydrogen bond network with both water molecules and other residues (Figure 1). The active site base (Ser175 in the *E. coli*

†This work was supported by National Institutes of Health Grant GM61087 to B.A.P. R.L.F. was supported by National Institute of General Medical Sciences Training Grant GM07767 and University of Michigan Rackham Graduate School Predoctoral Fellowship.

*To whom correspondence should be addressed: Department of Biochemistry, University of Iowa, 51 Newton Rd., Iowa City, IA 52242-1109. Phone: (319) 335-7775. Fax: (319) 335-7932. E-mail: rebecca-fagan@uiowa.edu.

[1]Abbreviations: DHOD, dihydroorotate dehydrogenase; DHO, dihydroorotate; OA, orotate; k_{red}, reduction rate constant; PDB, Protein Data Bank.

Published on Web 08/20/2009

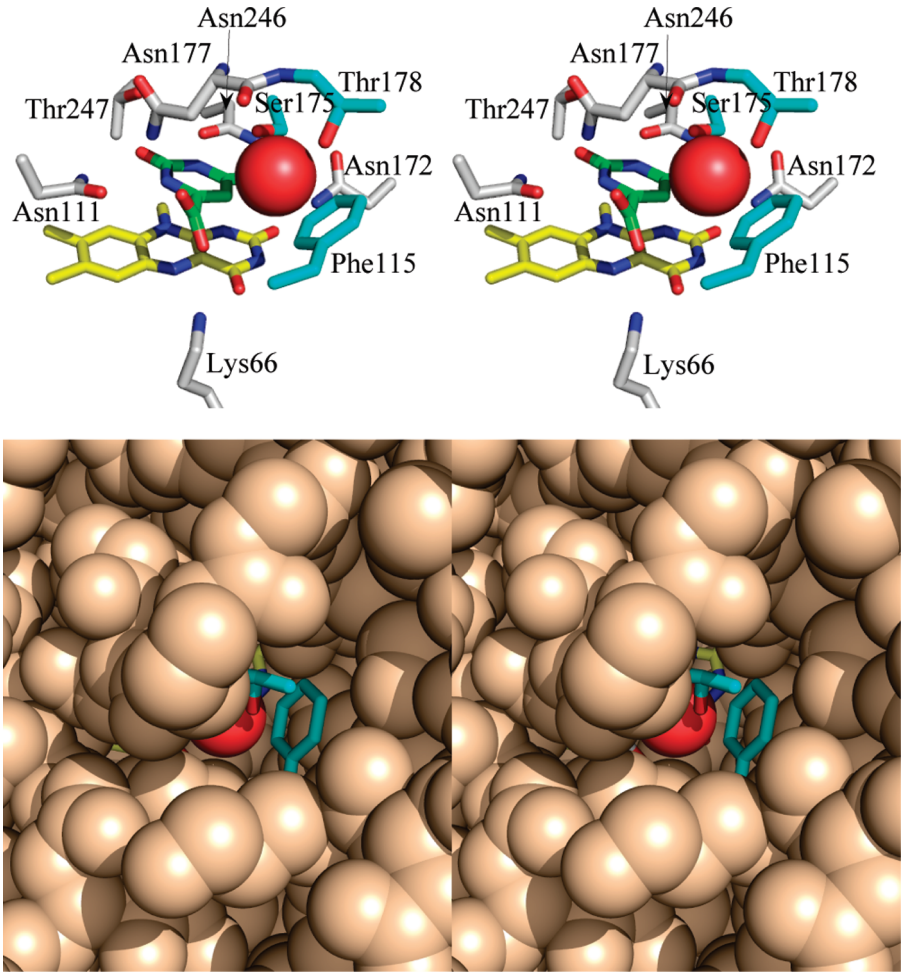

FIGURE 1: Stereoview of the hydrogen bond network to the pyrimidine-binding site of class 2 DHOD from *E. coli*. The top panel shows the active site base (Ser175), connected to the bulk solvent via a hydrogen bond network. A crystallographic water (red ball) sits on Phe115 and hydrogen bonds to Thr178, residues that are conserved in class 2 DHODs. In addition, the pyrimidine-binding site includes several highly conserved residues that hydrogen bond with the pyrimidine (OA colored green). The bottom panel highlights the small tunnel containing the hydrogen bond network. The viewpoint is from the right side of the top panel. Thr178 and Phe115 are shown as sticks; the crystallographic water is shown as a red sphere, and the rest of the protein is rendered as a space-filling diagram. Coordinates taken from PDB entry 1f76.

Scheme 1

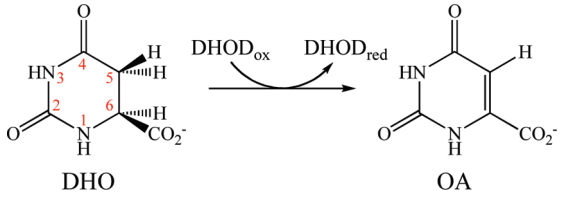

enzyme) hydrogen bonds to a crystallographic water that sits on a phenylalanine (Phe115 in the *E. coli* enzyme) and hydrogen bonds to a threonine (Thr178 in the *E. coli* enzyme), residues that are strictly conserved in class 2 DHODs. This hydrogen bond network connects the active site base to bulk solvent through a small tunnel. This network has been proposed to shuttle protons from the active site to bulk solvent and could have a role in allowing the serine to act as a base (*13*).

To investigate the role of this hydrogen bond network in DHO oxidation, site-directed mutants of the strictly conserved residues Ser175, Thr178, and Phe115 were created and the pH dependencies of their reductive half-reactions were determined. Blocking the tunnel and/or making the tunnel more hydrophobic impairs flavin reduction and supports the proposed role of this hydrogen bond network in flavin reduction.

EXPERIMENTAL PROCEDURES

Site-Directed Mutagenesis. Site-directed mutants were made from the previously created pAG-1 expression vector (*14*) using the Stratagene QuikChange II XL mutagenesis kit. Insertion of the correct mutations was checked by sequencing the entire pyrD gene.

Overexpression and Purification. All mutant enzymes were overexpressed from the pAG-1 plasmid in SØ6645 *E. coli* cells (*14*). The enzymes were purified according to the published procedure (*14*). Purified enzyme was diluted to 50% (v/v) with glycerol and stored at −80 °C. Before being used, enzymes were exchanged into the appropriate buffer using Econo-Pac 10DG disposable desalting columns (Bio-Rad).

Instrumentation. Absorbance spectra were recorded using a Shimadzu UV-2501PC scanning spectrophotometer. Stopped-flow experiments were performed at 4 °C using a Hi-Tech Scientific KinetAsyst SF-61 DX2 stopped-flow spectrophotometer.

Preparation of Anaerobic Solutions. Enzyme solutions for rapid reaction studies were made anaerobic in glass tonometers by repeated cycles of evacuation and equilibration over an atmosphere of purified argon as previously described (*15*). Substrate solutions were made anaerobic within syringes by being

Scheme 2

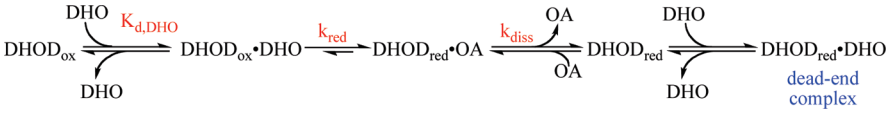

bubbled with purified argon before they were loaded onto the stopped-flow instrument. Slow reactions were performed in anaerobic cuvettes (*16*) and monitored in a standard scanning spectrophotometer. These reaction mixtures were also made anaerobic by repeated evacuation and equilibration with purified argon.

Reduction Potentials. Reduction potentials were determined by the xanthine/xanthine oxidase method of Massey (*17*). Experiments were performed in anaerobic cuvettes (*16*) and monitored in a standard scanning spectrophotometer at 25 °C and pH 7.0. Phenosafranin (E_m = −252 mV) was used as the indicator dye.

OA Binding to Oxidized Mutants. The dissociation constant of OA was determined in aerobic titrations in a standard scanning spectrophotometer. The enzyme equilibrated in 0.1 M Tris-HCl (pH 8.5) at 25 °C was titrated with OA in the same buffer. The differences in flavin absorbance caused by binding were plotted versus OA concentration, and the data were fit to eq 1

$$\Delta A = \Delta\varepsilon_{max}\left[\frac{E_0+L_0+K_d-\sqrt{(E_0+L_0+K_d)^2-4E_0L_0}}{2}\right] \quad (1)$$

where E_0 is the total enzyme concentration and L_0 is the total added ligand concentration, in Kaleidagraph (Synergy, Inc.) to determine the K_d.

pH Dependence of the Reduction of Mutant DHODs. The reductive half-reactions of the Thr178 and Phe115 single and double mutant enzymes were studied in anaerobic stopped-flow experiments at 4 °C. In most cases, the enzyme was equilibrated in 0.1 M buffer (pH 6−7.5, potassium phosphate; pH 7.5−9, Tris-HCl; pH 9−9.5, CHES; pH 10−11.5, CAPS) and mixed with varying concentrations of DHO in the same buffer. For the Phe115Leu and Phe115Leu/Thr178Val mutant enzymes, double-mixing pH-jump experiments were conducted at pH values higher than 10.5 due to enzyme instability. In these cases, the enzyme, equilibrated in 5 mM potassium phosphate (pH 7), was mixed with 0.2 M buffer (pH 10.5−11.5, CAPS) and allowed to age for 2 s. Then the enzyme was mixed with varying concentrations of DHO in 0.1 M buffer (pH 10.5−11.5, CAPS). In all cases, reaction traces were collected at 475 and 550 nm and were fit to sums of exponentials in Program A (R. Chang, C.-J. Chiu, J. Dinverno, and D. P. Ballou, University of Michigan). The reduction rate constant (k_{red}) at each pH value was determined from the limiting value of the observed rate constant at a saturating DHO concentration. This was obtained by fitting k_{obs} versus DHO concentration to a hyperbola in Kaleidagraph (Synergy, Inc.). For the Phe115Leu mutant enzyme at pH 8.5, the reaction traces could not easily be fit to sums of exponentials and were therefore analyzed by global fitting in Berkeley Madonna. Reaction traces at each concentration were averaged, and the average reaction traces for all concentrations were simultaneously fit to the mechanism in Scheme 2 (the scheme that describes the reductive half-reaction of wild-type *E. coli* DHOD). The rate constants used for binding of DHO to the oxidized and reduced enzyme were held constant during the fit to the values that describe the wild-type reaction. Both these steps are very fast and are not observed in our kinetic data. The initial estimates of the rate constants for flavin reduction and product dissociation were 2 s^{-1}. The model used for fitting is available as Supporting Information.

The pH dependence of flavin reduction was fit to a model in which only the deprotonated form of the enzyme reacts. This is described by eq 2

$$k_{red} = \frac{k_{red,limiting}}{1+10^{pK_a-pH}} \quad (2)$$

where $k_{red,limiting}$ (the limiting reduction rate constant at high pH) is the rate constant of the deprotonated form of the enzyme.

Reduction of the flavin in the Ser175Ala mutant DHOD was very slow at 4 °C; therefore, it was studied at 25 °C. The same buffers described above were used to investigate the pH dependence of flavin reduction in this enzyme. Below pH 9, flavin reduction was slow enough to be monitored using a standard scanning UV−vis spectrophotometer. Enzyme equilibrated in the buffer of interest was mixed with either 1 or 2 mM DHO (concentrations after mixing) in an anaerobic cuvette, and spectra were recorded at intervals until flavin reduction was complete. Reaction traces at 475 nm were extracted and fit to a single exponential. The observed rate constant at each DHO concentration was the same, indicating saturation. Since a saturating DHO concentration was used in each experiment, the k_{obs} obtained from fitting the exponential traces is equivalent to k_{red}. Above pH 9, the reductive half-reaction was investigated in anaerobic stopped-flow experiments. Anaerobic enzyme was mixed with varying concentrations of anaerobic DHO. Reaction traces were collected at 475 nm and fit to a single exponential. The reduction rate constant (k_{red}) was determined from the limiting value of the observed rate constant at saturating DHO concentrations obtained by fitting k_{obs} versus DHO concentration to a hyperbola in Kaleidagraph (Synergy, Inc.).

Solvent Isotope Effect. The solvent isotope effect on the reductive half-reaction of the wild-type enzyme was determined in anaerobic stopped-flow experiments at 4 °C using the methods described above for the pH dependence of the reductive half-reaction. Enzyme was equilibrated in 0.1 M potassium phosphate with either H_2O or D_2O as the solvent using a desalting column pre-equilibrated in that buffer. The pH of the buffer in H_2O was 7.7. For buffer in heavy water, potassium phosphate in H_2O was dried in vacuo, dissolved in D_2O, dried again, and redissolved in D_2O, thus maintaining the ratio of monobasic and dibasic phosphate present in the H_2O buffer.

RESULTS

Reduction Potentials. The reduction potential of the enzyme-bound flavin in the mutant enzymes was determined by the method of Massey (*17*) using phenosafranin as the indictor dye (Table 1 and Figure 2). The potential of the wild-type enzyme was recently reported to be −229 mV (*22*). The only mutation not to affect the reduction potential was Phe115Ala. All other mutations lowered the reduction potential. The largest effects were

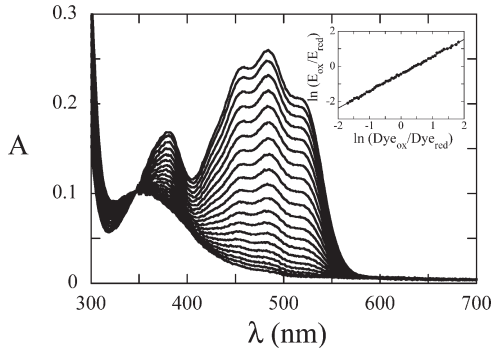

FIGURE 2: Determination of the reduction potential of Phe115Leu mutant DHOD. Phenosafranin was used as an indicator dye to determine the reduction potential. The inset shows the Nernst plot for determining the potential.

Table 1: Reduction Potentials of Mutant DHODs

enzyme	reduction potential[a] (mV)	enzyme	reduction potential[a] (mV)
wild type[b]	−229	Phe115Ala	−229
Ser175Ala	−267	Phe115Leu	−245
Thr178Ser	−249	Phe115Trp	−258
Thr178Ala	−269	Phe115Leu/Thr178Val	−239
Thr178Val	−264		

[a]Reduction potentials determined by the xanthine/xanthine method have a precision of ±5 mV. [b]Data taken from ref 22.

Table 2: Binding of OA to Oxidized Mutant DHODs at pH 8.5 and 25 °C

enzyme	K_d (μM)	enzyme	K_d (μM)
wild type[a]	3.4 ± 0.8	Phe115Ala	3.8 ± 0.5
Ser175Ala	9.9 ± 0.9	Phe115Leu	3.7 ± 0.3
Thr178Ser	1.1 ± 0.4	Phe115Trp	8.1 ± 0.4
Thr178Ala	6.1 ± 0.8	Phe115Leu/Thr178Val	4.6 ± 0.3
Thr178Val	0.56 ± 0.04		

[a]Data taken from ref 22.

seen in the Ser175Ala, Thr178Ala, and Thr278Val mutant enzymes. These enzymes had reduction potentials near −270 mV, ~40 mV lower than that of the wild type. Curiously, during the reduction of the Phe115Leu/Thr178Val double mutant, a small amount of neutral semiquinone was produced. Nonetheless, the Nernst plot was linear, and a two-electron potential for the enzyme could be determined.

OA Binding. Oxidized DHOD from *E. coli* has a maximum visible absorbance peak at 456 nm. The UV−vis absorbance spectra of all oxidized mutant enzymes were essentially identical to that of the wild type. Ligand binding often causes spectral perturbation in flavoenzymes. OA binding to oxidized DHODs causes a large red shift in the flavin absorbance (*14*, *18*−*22*). In the class 2 enzyme from *E. coli*, this shift is from 456 to 475 nm (*14*). By tracking this spectral change, we could determine the dissociation constant for OA in aerobic titrations at pH 8.5 and 25 °C (Figure 3). Similar spectral shifts were seen in all mutant enzymes, and only minor effects on K_d were observed (Table 2).

pH Dependence of Flavin Reduction. The reductive half-reaction of the class 2 DHOD from *E. coli* has been studied in great detail in anaerobic stopped-flow experiments (*11*, *12*). To probe the role of conserved residues in a hydrogen bond network connecting the active site base to bulk solvent, site-directed mutagenesis was used. Thr178, which hydrogen bonds to a

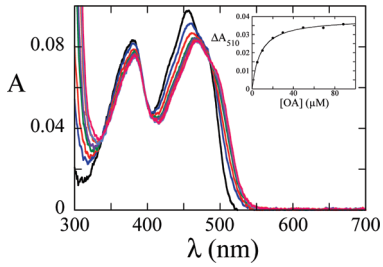

FIGURE 3: OA binding titration at pH 8.5 and 25 °C. The Phe115Ala mutant DHOD was titrated aerobically with OA. Upon OA binding, the maximum flavin peak shifts to the red. The inset shows the maximum change in absorbance due to OA binding as a function of OA concentration. Fitting to eq 1 gives the K_d value for OA (3.8 ± 0.5 μM).

crystallographic water in this network (Figure 1), was replaced with serine, alanine, and valine (the residue found in class 1A DHODs, which do not contain this network). The water sits on Phe115, which was replaced with alanine, leucine (the residue found in class 1A DHODs), and tryptophan. The reductive half-reaction of each of these mutant enzymes was studied in anaerobic stopped-flow experiments. In addition, the Phe115-Leu/Thr178Val double mutant enzyme was also studied. Data from all mutant enzymes fit the same scheme proposed for the wild-type enzyme (*11*) (Scheme 2). While the reductive half-reaction of the wild-type enzyme has been shown to be reversible, the equilibrium lies far toward the reduced enzyme and the rate constant for the reverse reaction (the reduction of OA to DHO) is so small compared to the rate constant for DHO oxidation that it is essentially zero (*11*). The same is true for the mutant enzymes studied here.

The spectral changes observed during the reductive half-reactions of the mutant enzymes were identical to those observed in the wild type (*11*, *12*). In most cases, DHO binding was very rapid and occurred during the dead time of the stopped-flow instrument. The Phe115Leu/Thr178Val double mutant enzyme displayed a very small first phase (over within the first 5 ms) that might be due to substrate binding. DHO binding is accompanied by a large shift in the flavin absorbance peak, from 456 to 475 nm. This spectral shift resembles the shift observed upon OA binding. The first phase observed in the double mutant consisted of a small increase at 510 nm (the wavelength at which the largest change is observed in the flavin spectrum upon OA binding), a small decrease at 450 nm, and a lag at 475 nm, all consistent with a spectral shift from 456 to 475 nm due to substrate binding. However, these spectral changes were very small and difficult to fit. Reliable rate constants for this phase could not be obtained.

In most DHODs, the wild type (*11*, *12*) and most mutant (*22*) class 2 enzymes as well as wild-type class 1A enzymes (*23*), the first observable phase in the reductive half-reaction is the chemical step, the reduction of the enzyme-bound flavin since substrate binding occurs during the dead time of the stopped-flow instrument. The same is true for all the mutants studied here except for the Phe115Lue/Thr178Val double mutant enzyme. The rate constant for flavin reduction is pH-dependent in DHODs (*11*, *12*, *23*). When the rate constant for flavin reduction is higher than that for product dissociation, the concentration of the reduced enzyme·OA complex that accumulates is large enough to be seen spectroscopically. When this occurs, flavin reduction, seen as a large decrease in absorbance at 475 nm, is accompanied by a concomitant increase in absorbance at 550 nm (Figure 4A). The 550 nm absorbance is due to a charge-transfer

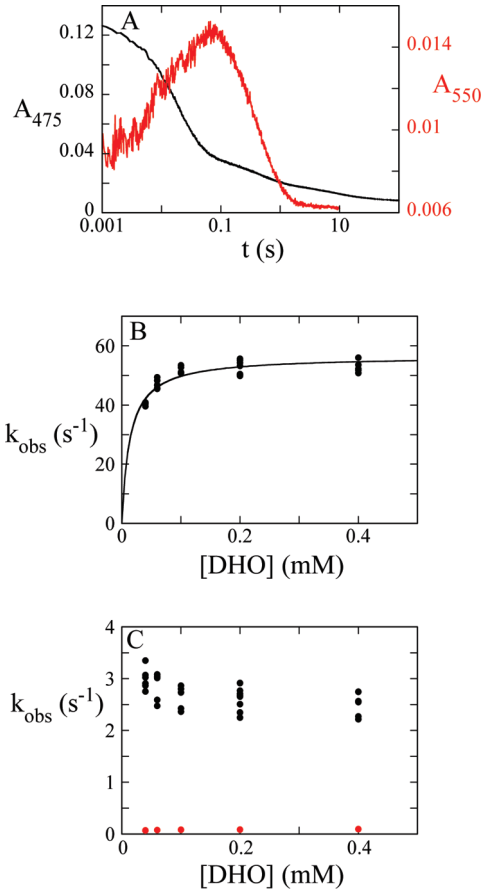

FIGURE 4: Reductive half-reaction of the Phe115Leu mutant DHOD at pH 10. (A) Enzyme (~9.5 μM after mixing) was mixed with DHO (400 μM after mixing) in an anaerobic stopped-flow experiment at 4 °C. The dead time of the stopped-flow instrument was 1 ms. At 475 nm (black), the reaction occurs in three phases. The first (large) phase represents the chemical step. The second phase represents product release. At 550 nm (red), flavin reduction is seen as an increase in absorbance and product dissociation is seen as a decrease in absorbance. Reaction traces are shown on a log scale. (B) The observed rate constant of the first phase (flavin reduction) saturates with an increasing DHO concentration, giving a reduction rate constant (k_{red}) of 56.5 ± 0.9 s^{-1} and an estimate for the $K_{d,DHO}$ of 14 ± 2 μM. (C) The observed rate constant of the second phase (black), OA release, decreases with an increasing DHO concentration, giving a limiting value of 2.5 s^{-1}. The observed rate constant of the final phase (red) is ~0.08 s^{-1} and is independent of DHO concentration.

interaction between the electron-rich reduced flavin and the electron-deficient OA. The following phase is caused by product dissociation and is accompanied by a decrease in absorbance at both 475 and 550 nm (Figure 4A). When flavin reduction is slower than product release, the reduced enzyme·OA complex does not accumulate and only flavin reduction is observed spectroscopically.

In all the mutant enzymes studied, a small final well-resolved phase representing < 10% of the total absorbance change was observed at 475 nm (Figure 4A). This phase was also observed in the wild type (*11*). It is unclear what this phase represents. It has been suggested that this phase could be due to the reduction of a small amount of contaminating free flavin (*11*) or slow reduction of damaged enzyme (*22*). The difference between the absorbance spectrum at the start of this slow phase and after its completion for the Phe115Leu/Thr178Val double mutant enzyme indicated that the reaction was the reduction of the red-shifted enzyme, suggesting that for this enzyme, the phase was due to the damaged enzyme.

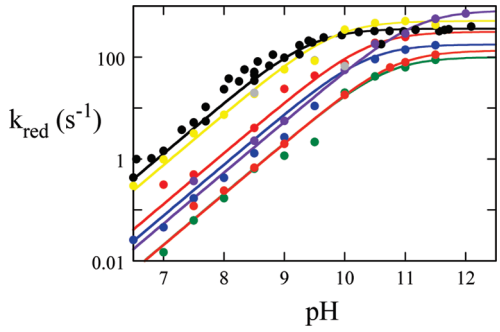

FIGURE 5: pH dependence of reduction rate constants: black for the wild type (*11*), yellow for Thr178Ser, blue for Thr178Ala, green for Thr178Val, red for Phe115Ala, purple for Phe115Leu, gray for Phe115Trp, and orange for Phe115Leu/Thr178Val. The limiting reduction rate constants and observed pK_a values can be found in Table 3.

The reaction traces obtained at 475 and 550 nm were fit to sums of exponentials. The observed rate constant of the phase representing flavin reduction saturated with increasing DHO concentrations. The reduction rate constant (k_{red}), the rate constant at an infinite DHO concentration, was determined by fitting the observed rate constant versus DHO concentration plot to a hyperbola (Figure 4B). The half-saturating value gives the apparent K_d of DHO. The observed rate constant of the product release phase decreased with an increasing DHO concentration (Figure 4C) as seen in the wild type (*11*). This concentration dependence indicates a unimolecular step (product release) followed by a bimolecular step (free reduced enzyme binding the unreacted DHO to form a reduced enzyme·DHO dead-end complex). The observed rate constant of the final phase was independent of DHO concentration and at least 1 order of magnitude smaller than the rate constants of the other phases (Figure 4C).

As mentioned earlier, the rate constant for flavin reduction increases with pH. The class 2 DHOD from *E. coli* exhibits a pK_a of ~9.5 (*11*). The pH dependence of the reduction rate constant was determined for the mutant enzymes[2] (Figure 5). In most cases, the reduction rate constant increased until reaching a break point on a log plot, indicating a pK_a. In some cases, flavin reduction was very fast at high pH, making it difficult to obtain accurate rate constants. In addition, the Phe115Leu mutant enzyme was unstable at high pH. Even during pH-jump experiments, a small percentage of the enzyme was denatured before reduction, further complicating the determination of accurate rate constants. Therefore, the values listed in Table 3 are the best estimates for $k_{red,limiting}$ (the limiting rate constant for flavin reduction at high pH).

The most conservative mutation studied (Thr178Ser) resulted in a pH dependence nearly identical to that of the wild type. The limiting reduction rate constant was ~500 s^{-1} (~1.4-fold faster than that of the wild type). The observed pK_a was shifted by ~0.3 pH unit to ~9.8 (Table 3). Larger effects were observed when Thr178 was mutated to alanine and valine. The limiting reduction rate constants were ~2-fold lower than that of the wild-type enzyme. In addition, the observed pK_a values were shifted ~1 pH unit to 10.4 (Thr178Ala) and 10.7 (Thr178Val). The Phe115Ala mutant enzyme had a limiting rate constant near that of the wild type. However, the observed pK_a was shifted to ~10.4.

[2]The Phe155Trp mutant enzyme was studied at only two pH values, and therefore, a pK_a value was not obtained.

The largest change in the pK_a was observed in the Phe115Leu mutant enzyme. The limiting rate constant of this mutant is estimated to be ~800 s^{-1} (~2-fold faster than that of the wild type). The observed pK_a is shifted nearly 2 pH units to ~11.2. Interestingly, when both Phe115 and Thr178 were mutated, the mutant enzyme behaved like the Thr178Val single mutant. The Phe115Leu/Thr178Val mutant had a limiting reduction rate constant of 135 s^{-1} and a pK_a of ~10.8.

The apparent K_d of DHO is also pH-dependent in the wild type (*11*) and the mutant enzymes studied here. In the wild-type enzyme, the K_d is low (~20 μM) until the pH is increased above ~10, whereupon the K_d increases, giving a pK_a of ~10.3 (*11*). Almost all the mutant enzymes studied behaved similarly, with tight binding observed up to a pH of ~10 (Supporting Information). However, the Phe115Ala and the Phe115Trp mutant enzymes were quite different. The K_d of DHO for the Phe115Ala mutant enzyme, even at low pH, was in the range of hundreds of micromolar and was independent of pH. The Phe115Trp mutant enzyme was studied at only pH 8.5 and 10.0, but the apparent K_d was near 1 mM at both pH values, nearly 2 orders of magnitude above that of the wild type.

When enough reduced enzyme·OA complex accumulates during the reaction to be seen spectroscopically, the rate constant of product release can be determined. In the wild-type enzyme, between pH 6 and 12, the average rate constant for product release is ~0.35 s^{-1} (*11*, *12*). The same was observed in all the Thr178 mutant enzymes. In all instances where the rate constant for product release could be obtained, it ranged from ~0.2 to 0.6 s^{-1}, independent of pH. The Phe115 mutant enzymes behaved very differently. In the Phe115Ala mutant DHOD, product release was observed at pH >9. The rate constant (~8 s^{-1}) was independent of pH but was 1 order of magnitude larger than that of the wild type. In the Phe115Trp mutant enzyme, the rate constant of product release was also much faster (~3.5 s^{-1}) than that of the wild type at pH 10.5. The rate constants for product dissociation for the Phe115Leu single mutant and the Phe115Leu/Thr178Val double mutant enzymes were pH-dependent. For the single mutant, at lower pH (8−9.5), the rate constant was ~1 s^{-1}. However, as the pH increased, the rate constant decreased. At pH 12, the rate constant was only ~0.2 s^{-1}, near the values routinely obtained with the wild-type enzyme. The same general trend was observed for the double mutant. The rate constant was ~5−6 s^{-1} at lower pH (9.5−10) and decreased as the pH increased to a value of ~0.4 s^{-1} at pH 11.5.

The pH dependence of the reductive half-reaction was also studied for the Ser175Ala mutant enzyme, whose active site base has been removed. For this enzyme, flavin reduction was extremely slow at 4 °C and was therefore studied at 25 °C. At all pH values, a single reaction phase, representing flavin reduction, was observed. The reduction rate constant increased with an increase in pH, showing no observable pK_a (Figure 6).

Solvent Isotope Effects. The solvent isotope effect on the rate constant for flavin reduction of the wild-type enzyme was determined at pH 7.7 and 4 °C in anaerobic stopped-flow experiments. The limiting rate constant for flavin reduction obtained in H_2O was 18.5 ± 0.2 s^{-1}, consistent with the value previously reported (*11*). When D_2O was used as the solvent for buffer with an identical ratio of conjugate acid and conjugate base, a rate constant for flavin reduction of 20.2 ± 0.4 s^{-1} was obtained. Therefore, a slightly inverse solvent isotope effect (0.92 ± 0.03) was obtained. The minor deviation from unity indicates that exchangeable protons are not in flight during flavin reduction.

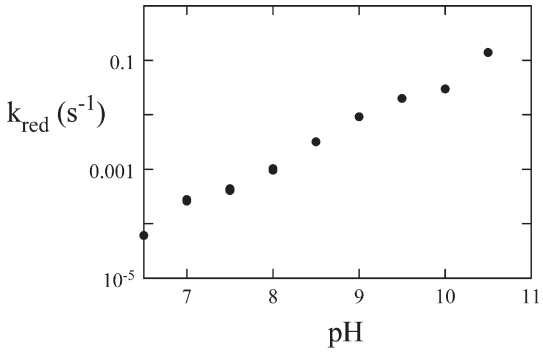

FIGURE 6: pH dependence of flavin reduction in the Ser175Ala mutant DHOD. The pH dependence was determined at 25 °C because the reaction was extremely slow at 4 °C. The reduction rate constant increases linearly on the log plot vs pH, with no indication of a pK_a.

DISCUSSION

DHODs catalyze the oxidation of DHO to OA using an active site base and a flavin prosthetic group. To oxidize DHO to OA, C5 must be deprotonated. Crystal structures of Class 2 DHODs show that a strictly conserved serine residue is properly positioned to act as an active site base (*7*−*9*). The pyrimidine-binding site of Class 2 DHODs is not exposed to solvent; therefore, the proton abstracted from C5 cannot go directly to the solvent. Instead, a hydrogen bond network connects the active site base to bulk solvent. In crystal structures, the active site base hydrogen bonds to a crystallographic water molecule that sits on a phenylalanine and hydrogen bonds to a threonine, strictly conserved residues in class 2 enzymes (*5*−*10*). Molecular dynamics studies have shown that a water molecule occupies the tunnel almost all of the time (*13*). Simulations were used to look for possible hydrogen bond networks; the same network observed in crystal structures was also found in the simulations (*13*). This pathway seems to be the most reasonable for transferring a proton to bulk solvent. The proton would be passed from C5 of DHO to the active site base (Ser175 in *E. coli* DHOD), to the water molecule in the tunnel, to a conserved threonine (Thr178 in *E. coli* DHOD), and finally to bulk solvent (Figure 1). In contrast, the active sites of class 1 enzymes are much more exposed to solvent (*19*, *24*−*27*), negating the need for a hydrogen bond network. Site-directed mutilation was used to probe the role of the conserved proton-relay network in the *E. coli* class 2 DHOD.

The mutations apparently had little effect on the pyrimidine-binding site and the flavin environment. The absorbance spectra of the oxidized enzymes were nearly identical to that of the wild type, with a maximum flavin peak at 456 nm. In addition, circular dichroism spectra of the flavin chromophore of oxidized and reduced mutant enzymes (Supporting Information) were roughly similar to those of the wild-type enzyme, indicating that the mutations caused only minor changes at most to the flavin environment. All the mutant enzymes exhibited the usual spectral shift in the flavin absorbance upon OA binding, indicating the pyrimidine-binding site is relatively unperturbed. The mutations also had little effect on the K_d of OA (Table 2), presumably because they are far from the binding site (*9*).

However, the reduction potentials of most of the mutants were lower than that of the wild type (Table 1). Reduction potentials report on the differential affinities of the apoenzyme for oxidized and reduced flavin. A decrease in potential could be caused by

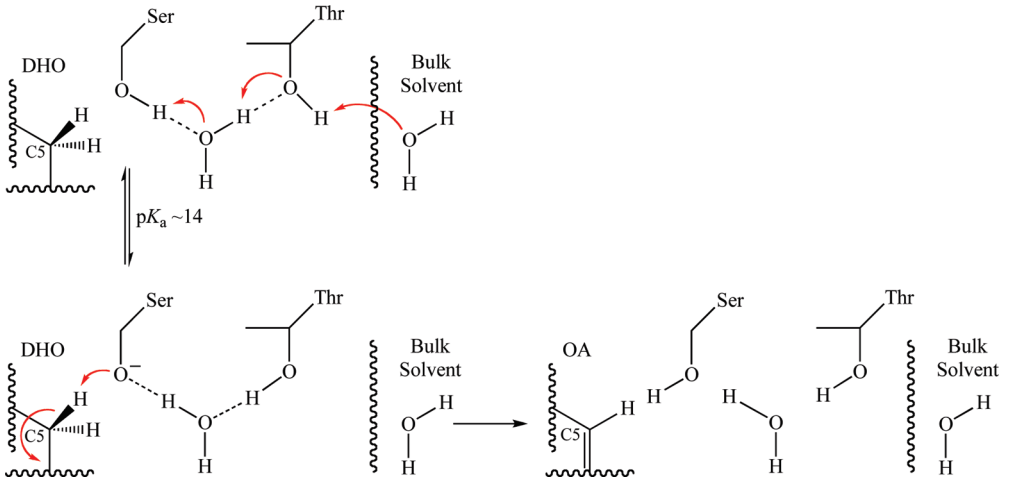

FIGURE 7: Proposed proton relay in class 2 DHODs. A small amount of the alkoxide form of Ser175 [the active site base, p$K_a \geq 14$ (*12*)] is generated by the proton relay network. The alkoxide form then deprotonates DHO in the redox reaction.

a tightening of the binding of oxidized FMN to the apoprotein, a weakening of the binding of reduced FMN, or perhaps a bit of each. The largest difference in reduction potentials between mutant and wild-type enzymes was 40 mV (Thr178Ala and Ser175Ala) or 1.8 kcal/mol, approximately the strength of a typical hydrogen bond. It is unclear why this occurs; the residues replaced are far from the flavin itself (*9*). Although decisive information is absent, it seems unlikely that these mutations, which disrupt hydrogen bonds in the protein, would strengthen the binding of oxidized flavin. Therefore, we tentatively favor the idea that the mutations have weakened the binding of reduced FMN.

Changes to the reductive half-reaction in the mutant enzymes were quantitative rather than qualitative. In all mutant enzymes, the reduction rate constant was pH-dependent, as it is in the wild type (*11*). In all mutant enzymes except Ser175Ala (where the active site base was removed), the reduction rate constant increased with an increase in pH until a plateau was reached, indicating a pK_a. In the wild type, the pK_a is ~9.5 (*11*). However, no structural features exist that could lower the pK_a of the active site serine (*7*−*9*). In fact, empirical calculations of the perturbation of the pK_a by the protein predict a slight increase in the pK_a of the base due to the protein environment, rather than a decrease (*12*). Kinetic isotope effect studies have shown that DHO oxidation in the *E. coli* DHOD is stepwise (*12*). The isotope effect contributed by deprotonating C5 disappears at a pH value above the pK_a (*12*), indicating that the observed pK_a is a kinetic rather than thermodynamic pK_a, caused by the rate of deprotonation becoming so high that it is no longer partially rate-determining.

The pH dependencies of each mutant and the wild-type enzyme fit well to a model in which only the deprotonated enzyme·DHO complex reacts. We have previously proposed that the reactive form of the enzyme is the small fraction of Ser175 in the alkoxide form (*12*). The data from this study indicate that the proton relay network is required to rapidly generate the small amount of alkoxide that is present near neutral pH (Figure 7). In this way, the network decouples the transfer of a proton to solvent from the deprotonation of DHO. This model explains the kinetic pK_a on the reduction rate constant. It also explains the lack of a solvent isotope effect on the reaction of the wild-type enzyme; the transfer of the exchangeable protons of the network (each with a fractionation factor expected to be ~1) is not part of the transition state of DHO deprotonation/oxidation. Instead, the exchangeable protons are proposed to move prior to the redox chemistry.

Table 3: pH Dependence on Flavin Reduction

enzyme	lim k_{red} (s^{-1})	pK_a
wild type[a]	360 ± 20	9.5 ± 0.1
Thr178Ser	~500	~9.8
Thr178Ala	180 ± 10	10.4 ± 0.1
Thr178Val	100 ± 4	10.7 ± 0.1
Phe115Ala	315 ± 20	10.4 ± 0.1
Phe115Leu	~800	~11.2
Phe115Leu/Thr178Val	135 ± 2	10.8 ± 0.1

[a]Data taken from ref 11.

When residues in the proton relay network were mutated, significant shifts were observed in the pK_a values (Table 3). The pK_a values observed in these enzymes are kinetic rather than thermodynamic. Above the pK_a, the rate constant for deprotonating C5 of DHO has become too fast to be partially rate determining. Residues were changed to increase or decrease the size of the tunnel and change the hydrophobicity of the tunnel. The higher kinetic pK_a values observed in the mutant enzymes imply that deprotonation of the active site base has become less efficient since higher pH values are required to make deprotonation too fast to be partially rate determining. When either Thr178 or Phe115 was mutated to alanine, the kinetic pK_a was nearly 1 pH unit higher than in the wild type. These mutations would increase the size of the tunnel, giving water more room to move, and thus make the hydrogen bond network less ordered. Decreasing the size of the tunnel and increasing the hydrophobicity had even greater effects. In the Thr178Val mutant enzyme, the pK_a shifted to ~10.7. Valine is isosteric with threonine, but more hydrophobic. Valine would block the tunnel, and its side chain would presumably need to move to accommodate water and allow proton transfer. An even larger effect is observed in the Phe115Leu mutant enzyme, in which the pK_a is shifted to ~11.2. Replacing phenylalanine (an aromatic side chain) with leucine (an aliphatic side chain) will increase the hydrophobicity of the local environment markedly. As a model, it is worth noting that the solubility of water in benzene is ~20 mM, while the solubility of water in hexane is ~10-fold lower (*28*). These data suggest that the mutation makes this area less hospitable for water.

Interestingly, in the Phe115Leu/Thr178Val double mutant enzyme, the values of pK_a and $k_{red,limiting}$ were nearly identical to those of the Thr178Val single mutant, indicating that mutation of Thr178 is dominant and the residues are not synergistic. Mutation of Phe115 has no effect in the absence of Thr178. This suggests that in the absence of its threonine hydrogen bonding partner, the water of the proton relay network becomes disordered regardless of the hydrophobicity of its cavity.

Hydrogen bonding pathways are very important for catalysis in many enzymes. Simulations have shown that the rate of proton transfer through hydrophobic channels can be increased by ~20-fold just by constraining water molecules to a single-file chain (*29*). Alcohol dehydrogenase contains a proton relay network responsible for deprotonating water or an alcohol ligated to the catalytic zinc. In this instance, the base, a histidine located at the surface of the enzyme, is connected to the active site zinc ligand via a hydrogen bond network. When the histidine is replaced with glutamine, the pK_a controlling alcohol oxidation is shifted ~3 pH units higher than that in the wild type (*30*). Proton relay networks are also known to play a major role in catalysis by cytochromes P450 (*31*, *32*). The important hydrogen bond networks contain both water molecules and protein residues. In wild-type crystal structures, well-ordered water molecules can be observed in the hydrogen bond networks. This is also seen in class 2 DHODs. However, in structures of mutant cytochromes P450 in which the hydrogen bond networks are perturbed, the water molecules either are not visible or have decreased occupancies, indicating that protein mutations can affect the number and timely availability of water molecules important for catalysis (*32*, *33*).

As mentioned earlier, DHO oxidation by class 2 DHODs is stepwise, and the observed pK_a is actually a kinetic pK_a (*12*). Above the pK_a, deprotonation is too fast to be partially rate determining. Thus, the rate constants obtained above the kinetic pK_a represent the rate constant of transfer of hydride from C6 of DHO to the flavin and should not be sensitive to an intact proton-transfer network. Mutating Phe115 had little effect on $k_{red,limiting}$ (Table 3); above the observed pK_a, the rate constant was very high. However, mutation of the Thr178 to either alanine or valine reduced the rate constant observed above the pK_a by 2−3-fold compared to that of the wild-type enzyme. This indicates that removing the OH group from position 178 affects the rate constant of transfer of a hydride to FMN as well as disordering the hydrogen bond network. Thr178 is next to Asn177. Asn177, a strictly conserved residue that hydrogen bonds to the carboxylate of DHO, is thought to be responsible in part for orienting DHO for catalysis (*22*). It is possible that disordering the hydrogen bond network also partially disorders Asn177, thereby reducing the rate constant of hydride transfer due to improper positioning of DHO.

The pH dependence of flavin reduction was also studied for the Ser175Ala mutant enzyme to investigate the function of the active site base. In this enzyme, reduction was extremely slow and thus was studied at 25 °C to speed the reaction. The reduction rate constant was pH-dependent, as in all other mutants, but there was no observable pK_a up to pH 10.5 (Figure 6). The active site base mutant of the class 1A DHOD from *Lactococcus lactis* (Cys130Ala) has been previously studied at 25 °C (*23*), allowing a direct comparison with the data presented here. The reduction rate constant of the Ser175Ala mutant enzyme was at least 1 order of magnitude faster than that of the Cys130Ala mutant enzyme at all pH values investigated. In both these enzymes, a water molecule occupying the cavity opened by mutation likely acts as the base. The class 2 enzyme is better able to catalyze the reaction without its active site base than the class 1A enzyme is. This is probably due to the presence of the proton relay network in class 2 enzymes, which would be properly positioned to shuttle a proton from the active site, even if it is from a disordered water molecule acting as a base.

The reductive half-reaction of DHODs demands a route for removal of a proton. Class 1A enzymes, which have much more solvent-exposed active sites, presumably do this by direct reaction with solvent. However, a hydrogen bond network is needed to accomplish this in class 2 DHODs. In these enzymes, the active site serine alone is not sufficient. The entire ordered proton relay network is needed for the most effective deprotonation of DHO.

SUPPORTING INFORMATION AVAILABLE

Flavin CD spectra of oxidized and reduced wild-type and mutant enzymes, pH dependence of the apparent $K_{d,DHO}$, and the Berkley Madonna global fitting simulation for the reductive half-reaction of the Phe115Leu mutant enzyme at pH 8.5. This material is available free of charge via the Internet at http://pubs.acs.org.

REFERENCES

1. Björnberg, O., Rowland, P., Larsen, S., and Jensen, K. F. (1997) Active site of dihydroorotate dehydrogenase A from *Lactococcus lactis* investigated by chemical modification and mutagenesis. *Biochemistry 36*, 16197–16205.
2. Jones, M. E. (1980) Pyrimidine nucleotide biosynthesis in animals: Genes, enzymes, and regulation of UMP biosynthesis. *Annu. Rev. Biochem. 49*, 253–279.
3. Nagy, M., Lacroute, F., and Thomas, D. (1992) Divergent evolution of pyrimidine biosynthesis between anaerobic and aerobic yeasts. *Proc. Natl. Acad. Sci. U.S.A. 89*, 8966–8970.
4. Nielsen, F. S., Andersen, P. S., and Jensen, K. F. (1996) The B form of dihydroorotate dehydrogenase from *Lactococcus lactis* consists of two different subunits, encoded by the pyrDb and pyrK genes, and contains FMN, FAD, and [FeS] redox centers. *J. Biol. Chem. 271*, 29359–29365.
5. Baumgartner, R., Walloschek, M., Kralik, M., Gotschlich, A., Tasler, S., Mies, J., and Leban, J. (2006) Dual binding mode of a novel series of DHODH inhibitors. *J. Med. Chem. 49*, 1239–1247.
6. Hansen, M., Le Nours, J., Johansson, E., Antal, T., Ullrich, A., Loffler, M., and Larsen, S. (2004) Inhibitor binding in a class 2 dihydroorotate dehydrogenase causes variations in the membrane-associated N-terminal domain. *Protein Sci. 13*, 1031–1042.
7. Hurt, D. E., Widom, J., and Clardy, J. (2006) Structure of *Plasmodium falciparum* dihydroorotate dehydrogenase with a bound inhibitor. *Acta Crystallogr. D62*, 312–323.
8. Liu, S., Neidhardt, E. A., Grossman, T. H., Ocain, T., and Clardy, J. (2000) Structures of human dihydroorotate dehydrogenase in complex with antiproliferative agents. *Structure 8*, 25–33.
9. Nørager, S., Jensen, K. F., Björnberg, O., and Larsen, S. (2002) *E. coli* dihydroorotate dehydrogenase reveals structural and functional distinctions between different classes of dihydroorotate dehydrogenases. *Structure 10*, 1211–1223.
10. Walse, B., Dufe, V. T., Svensson, B., Fritzson, I., Dahlberg, L., Khairoullina, A., Wellmar, U., and Al-Karadaghi, S. (2008) The structures of human dihydroorotate dehydrogenase with and without inhibitor reveal conformational flexibility in the inhibitor and substrate binding sites. *Biochemistry 47*, 8929–8936.
11. Palfey, B. A., Björnberg, O., and Jensen, K. F. (2001) Insight into the chemistry of flavin reduction and oxidation in *Escherichia coli* dihydroorotate dehydrogenase obtained by rapid reaction studies. *Biochemistry 40*, 4381–4390.
12. Fagan, R. L., Nelson, M. N., Pagano, P. M., and Palfey, B. A. (2006) Mechanism of flavin reduction in class 2 dihydroorotate dehydrogenases. *Biochemistry 45*, 14926–14932.

13. Small, Y. A., Guallar, V., Soudackov, A. V., and Hammes-Schiffer, S. (2006) Hydrogen bonding pathways in human dihydroorotate dehydrogenase. *J. Phys. Chem. B 110*, 19704–19710.
14. Björnberg, O., Gruner, A. C., Roepstorff, P., and Jensen, K. F. (1999) The activity of *Escherichia coli* dihydroorotate dehydrogenase is dependent on a conserved loop identified by sequence homology, mutagenesis, and limited proteolysis. *Biochemistry 38*, 2899–2908.
15. Palfey, B. A. (2003) Time Resolved Spectral Analysis. In Kinetic Analysis of Macromolecules (Johnson, K. A., Ed.) pp 203−227, Oxford Unversity Press, New York.
16. Williams, C. H. Jr., Arscott, L. D., Matthews, R. G., Thorpe, C., and Wilkinson, K. D. (1979) Methodology employed for anaerobic spectrophotometric titrations and for computer-assisted data analysis. *Methods Enzymol. 62*, 185–198.
17. Massey, V. (1990) A simple method for the determination of redox potentials. In Flavins and Flavoproteins (Curti, B., Ronchi, S., and Zanetti, G., Eds.) pp 59−66, Walter de Gruyter, Berlin.
18. Marcinkeviciene, J., Jiang, W., Locke, G., Kopcho, L. M., Rogers, M. J., and Copeland, R. A. (2000) A second dihydroorotate dehydrogenase (Type A) of the human pathogen *Enterococcus faecalis*: Expression, purification, and steady-state kinetic mechanism. *Arch. Biochem. Biophys. 377*, 178–186.
19. Nørager, S., Arent, S., Björnberg, O., Ottosen, M., Lo Leggio, L., Jensen, K. F., and Larsen, S. (2003) *Lactococcus lactis* dihydroorotate dehydrogenase A mutants reveal important facets of the enzymatic function. *J. Biol. Chem. 278*, 28812–28822.
20. Wolfe, A. E., Thymark, M., Gattis, S. G., Fagan, R. L., Hu, Y. C., Johansson, E., Arent, S., Larsen, S., and Palfey, B. A. (2007) Interaction of benzoate pyrimidine analogues with class 1A dihydroorotate dehydrogenase from *Lactococcus lactis*. *Biochemistry 46*, 5741–5753.
21. Zameitat, E., Pierik, A. J., Zocher, K., and Loffler, M. (2007) Dihydroorotate dehydrogenase from *Saccharomyces cerevisiae*: Spectroscopic investigations with the recombinant enzyme throw light on catalytic properties and metabolism of fumarate analogues. *FEMS Yeast Res. 7*, 897–904.
22. Fagan, R. L., and Palfey, B. A. (2009) Roles in Binding and Chemistry for Conserved Active Site Residues in the Class 2 Dihydroorotate Dehydrogenase from *Escherichia coli*. *Biochemistry 48*, 7169–7178.
23. Fagan, R. L., Jensen, K. F., Björnberg, O., and Palfey, B. A. (2007) Mechanism of flavin reduction in the class 1A dihydroorotate dehydrogenase from *Lactococcus lactis*. *Biochemistry 46*, 4028–4036.
24. Arakaki, T. L., Buckner, F. S., Gillespie, J. R., Malmquist, N. A., Phillips, M. A., Kalyuzhniy, O., Luft, J. R., Detitta, G. T., Verlinde, C. L., Van Voorhis, W. C., Hol, W. G., and Merritt, E. A. (2008) Characterization of *Trypanosoma brucei* dihydroorotate dehydrogenase as a possible drug target: Structural, kinetic and RNAi studies. *Mol. Microbiol. 68*, 37–50.
25. Inaoka, D. K., Sakamoto, K., Shimizu, H., Shiba, T., Kurisu, G., Nara, T., Aoki, T., Kita, K., and Harada, S. (2008) Structures of *Trypanosoma cruzi* dihydroorotate dehydrogenase complexed with substrates and products: Atomic resolution insights into mechanisms of dihydroorotate oxidation and fumarate reduction. *Biochemistry 47*, 10881–10891.
26. Rowland, P., Björnberg, O., Nielsen, F. S., Jensen, K. F., and Larsen, S. (1998) The crystal structure of *Lactococcus lactis* dihydroorotate dehydrogenase A complexed with the enzyme reaction product throws light on its enzymatic function. *Protein Sci. 7*, 1269–1279.
27. Rowland, P., Nørager, S., Jensen, K. F., and Larsen, S. (2000) Structure of dihydroorotate dehydrogenase B: Electron transfer between two flavin groups bridged by an iron-sulphur cluster. *Structure 8*, 1227–1238.
28. Wolfenden, R., and Radzicka, A. (1994) On the probability of finding a water molecule in a nonpolar cavity. *Science 265*, 936–937.
29. Voth, G. A. (2006) Computer simulation of proton solvation and transport in aqueous and biomolecular systems. *Acc. Chem. Res. 39*, 143–150.
30. LeBrun, L. A., Park, D. H., Ramaswamy, S., and Plapp, B. V. (2004) Participation of histidine-51 in catalysis by horse liver alcohol dehydrogenase. *Biochemistry 43*, 3014–3026.
31. Schlichting, I., Berendzen, J., Chu, K., Stock, A. M., Maves, S. A., Benson, D. E., Sweet, R. M., Ringe, D., Petsko, G. A., and Sligar, S. G. (2000) The catalytic pathway of cytochrome P450cam at atomic resolution. *Science 287*, 1615–1622.
32. Vidakovic, M., Sligar, S. G., Li, H., and Poulos, T. L. (1998) Understanding the role of the essential Asp251 in cytochrome P450cam using site-directed mutagenesis, crystallography, and kinetic solvent isotope effect. *Biochemistry 37*, 9211–9219.
33. Makris, T. M., von Koenig, K., Schlichting, I., and Sligar, S. G. (2007) Alteration of P450 distal pocket solvent leads to impaired proton delivery and changes in heme geometry. *Biochemistry 46*, 14129–14140.